Hensen's Stripe as a topographic waveguide defines the roles of the OHC & IHC[1]

Author: James T. Fulton

Address: c/o Hearing Concepts
1106 Sandpiper Dr.
Corona Del Mar, Calif 92625, USA

Telephone: 1-949-759-0630

E-Mail: Jtfulton@cox.net

Abstract:

The surgical literature suggests a direct acoustic connection between the oval window and Hensen's stripe on the gelatinous surface of the tectorial membrane (TM). Hensen's stripe can be described as a topographic waveguide. The curvature of such a topographic waveguide is known to control the dispersion of the energy as a function of frequency. Describing this curvature by a Hankel function, the propagation velocity by the data of Ghaffari et al., and employing the dispersion equation of Marcatili provides a complete description of the place-frequency-delay function of hearing for all species of mammals. The dispersion mechanism provides the first documented explanation of the very high attenuation versus frequency (exceeding 500 dB/octave) on the high frequency side of the best frequency in both OHC and IHC signaling channels. This attenuation is described by "an exponential of an exponential function." Such attenuations are not achievable by any other known mechanism. The resulting propagation and dispersion of energy explains the unique functional roles of both the OHC and IHC, and eliminates the need for any acousto-mechanical amplifier between the basilar membrane and the sensory neurons.

1. Introduction [2]

While a wide variety of localized models of the hearing processes carried out within the cochlear partition have been proposed, it is difficult to find one that describes the end-to end-processes between the oval window of the labyrinth and the mechanical excitation applied to the inner and outer hair cells. The two most common concepts of energy propagation within the cochlear partition exhibit major problems in the light of the known laws of physics. To overcome these problems, a comprehensive review of the literature was undertaken to find a plausible explanation for the overall process. The following material will present a contiguous model of the hearing process that is compatible with the surgical literature, explains the explicitly different roles played by the inner and outer hair cells, and for the first time provides an explanation for the unique attenuation characteristic associated with the high frequency roll-off of the neural signals derived from the cochlear partition.

Recent leaders in the field have predicted the tectorial membrane would assume the principle role in cochlear partition operation[1]. This paper confirms this prediction while focusing more precisely on the liquid-crystalline layer of the tectorial membrane and specifically Hensen's stripe.

The details of the work presented here has been reported in other publications and on the internet[2,3]. The latter source includes a series of animations that will be cited below. The goal of this paper is to provide an overview of that study. While the broader study explored hearing from a variety of perspectives, this paper will provide a sequential discussion of the hearing system beginning at the oval window of the vestibule of the labyrinth and ending with the application of acoustic energy to the cilia of the acoustic sensory neurons.

2. The operation of the vestibule of the labyrinth and cochlear partition

---

[1]Released: July 21, 2008

[2]Abbreviations: TM; tectorial membrane. OHC; outer hair cell. IHC; inner hair cell. LCL; liquid-crystalline layer of the tectorial membrane. SAW; surface acoustic wave. RC; resistor-capacitor. Q; quality factor =center frequency/ bandwidth of a narrow band circuit.

2 Mechanics of Hearing

Prior to the discussion of the operation of the acoustic elements of the labyrinth, it is appropriate to review the properties of the liquid crystalline surface of the tectorial membrane(TM). The TM is a complex laminated, structure. Its most important two laminates are the structure-free liquid-crystalline (gelatinous) layer (LCL) on its surface facing the reticular lamina of the basilar membrane, and the next laminate of the membrane supporting the liquid crystalline layer. The other surface, facing Reissner's membrane exhibits an entirely different structure that has caused it to be described as the reticulated, or preferably the net-covered, surface.

2.1 The properties of the liquid crystalline layer of the tectorial membrane

Kronester-Frei has described the tectorial membrane in detail[4,5], including the unique molecular-level structure of the surface of the tectorial membrane (TM) facing the sensory neurons. This gelatinous layer incorporates a longitudinal ridge labeled Hensen's stripe. She described Hensen's stripe as a specific feature of this surface, and as located directly opposite the IHC.

The following observation of Kronester-Frei is particularly important. "These investigations indicate, firstly, that the protofibrils of the tectorial membrane are very strongly influenced by changes in the ionic milieu. The reactions were so strong that morphological changes were visible and measurable. Under the influence of Na^+ ions, the protofibril system shrinks irreversibly, while during Ca^{2+} removal, it swells." The purpose of Reissner's membrane can be deduced from these comments; to provide a low sodium environment (endolymph in the scala media) that protects the liquid crystalline surface of the tectorial membrane from chemical attack by the perilymph.

Lim[6] has provided additional contemporary, and generally supportive, data to that of Kronester-Frei. Thalmann et al[7]. and Hasko & Richardson[8] have also contributed considerable new material expanding on the Kronester-Frei foundation. Thalmann et al. note the LCL has a wet weight consisting of 96.5% water and an amino acid composition similar to endolymph.

Zwislocki et al. explored the structural properties of the active surface of the tectorial membrane in 1988[9]. They noted the 1962 comment by Tonndorf et al., that the "tectorial membrane is 'springy' and not viscous." They further noted;
• "Manipulation of the tectorial membrane . . . has shown that the membrane is highly compliant in all directions"
•"The resulting deformation patterns have revealed that, under natural conditions, the tectorial membrane acts much more like a rubber band than a stiff board or a book cover. This is not consistent with the classical model of shear motion between the tectorial membrane and the reticular lamina," and
• "In addition, the high radial compliance of the membrane is not compatible with the [bending] mode of stereocilia deflection postulated in the model." The model referred to in both cases was the transverse endolymphatic fluid flow model of Allen.

While these statements are couched in the vernacular of the time, it is clear that the active surface of the tectorial membrane facing the reticular lamina exhibits very low compliance under static conditions. Figure 8A & 8B of their paper show the unique, structure-free, gel surface of the tectorial membrane and the underlying quasi-radial fibers. The point they missed was; the LCL brings a unique set of mechanical properties to the mechanism of acoustic energy propagation. Like any gel, it exhibits an unusual Poisson's ratio. Long term (at zero acoustic frequency), a gel cannot resist a tensile force and it will flow. However, it exhibits a finite Poisson's ratio at finite acoustic frequencies. As a result, the LCL exhibits negligible attenuation to surface acoustic waves with frequencies at least as high as any frequency found in biological hearing. Liquid-crystalline materials are often described as "ringing gels" in the lower level chemistry laboratories. Liquid crystals propagate acoustic energy without dispersion because of its crystalline lattice structure. Ghaffari et al. have recently confirmed the ability of the LCL of the *murine* tectorial membrane to propagate a low velocity acoustic wave[10]. While addressing only a Lamb-type SAW, they did document velocities of the surface wave (3-6 m/sec) over the audio frequency range in the LCL using a tectorial membrane and an artificial endolymph. The Lamb wave is a component of the modified Rayleigh wave described in Section 2.4.2.

2.2 The acoustic path between the vestibule and the cochlear partition

The hearing literature is remarkably silent concerning how acoustic energy from the oval window is propagated to the elements of the cochlear partition. Those supporting acoustic propagation in the scala vestibuli have assumed that the acoustic path must follow the fluid path defined by the presence of perilymph. This assumption has not been demonstrated. Those supporting acoustic propagation along the basilar membrane have been silent on how the energy is propagated from the oval window to the basilar membrane. The surgical literature, although limited in volume, has provided a clearer description of the acoustic propagation path between the oval window and the cochlear partition. The following two figures rely primarily upon the surgical information in Anson & Donaldson[11],

Figure 2.2.1-1 is assembled from several images of Anson & Donaldson. The elements of hearing outside the neural system have traditionally been divided into the outer ear, the middle ear, and the inner ear. This view shows the conventionally defined middle ear interfaces with the vestibule of the labyrinth rather than the scala vestibuli as generally assumed in the pedagogical and academic literature of hearing. Finally, it emphasizes the physical prominence of the extension of the cochlear partition (the caecum of the vestibule) within the vestibule and its location relative to the oval window. This prominence is crucial in the transfer of acoustic energy from the oval window to the tectorial membrane of the cochlear partition (**Section 2.2.2**). Page 267 shows the wall between the endolymph of the cochlear partition and the perilymph of the vestibule to be similar to Reissner's membrane. It has a thickness of only a few layers of cells. Thus, it offers negligible impedance to the transfer of acoustic energy compression waves between these two fluids. While the termination of the scala vestibuli in a cul-de-sac near the vestibule of the labyrinth was not explicitly presented in Anson & Donaldson, the cul-de-sac of the scala tympani is well documented and so-named.

The oval and round windows are the only access between the elements of the inner ear and the air-filled space of the middle ear in the terrestrial vertebrates. Notice the oval window and round window exhibit no unique orientation relative to the Organ of Corti. The acoustic energy is delivered to the common vestibule between the semicircular canals on the left and the cochlea on the right, via the stapes and oval window. The energy progresses from the oval window, through the perilymph of the vestibule, through the membrane labeled the caecum of the vestibule and into the scala media and the tectorial membrane.

This paper will subdivide the inner ear into two major elements. The portion between the oval window and the point just past the caecum of the vestibule where Hensen's stripe (described in the following figures) begins to curve in the plane of the cochlear partition will be described as stage C1 here. The portion of the inner ear between the start of the above curvature and the helicotrema will be defined as stage C2 or the active portion of the cochlear partition.

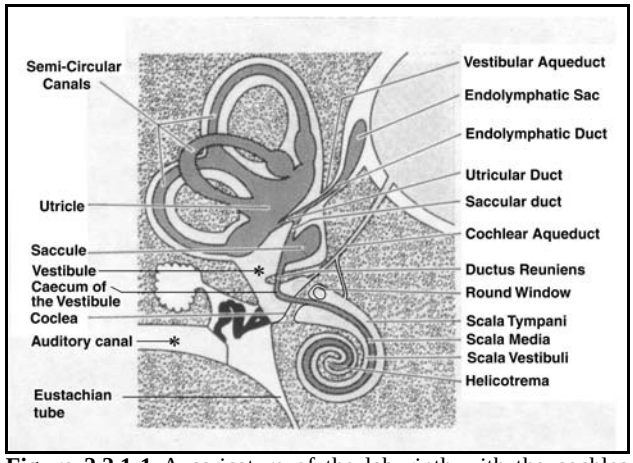

Figure 2.2.1-1 A caricature of the labyrinth with the cochlea acoustically isolated from the vestibule by bone, except for the access via the vestibular caecum (a.k.a. cul-de-sac of the cochlear partition or scala media). The cochlear partition is labeled the scala media in this image. The interpretation portrayed here agrees with the surgical record but not the conventional wisdom within the hearing community. Modified from an earlier caricature in Jahn & Santos-Sacchi, 1988.

2.2.1 Evolution and development of the cochlea and cochlear partition

Except for the active echolocators, the human cochlea is one of the most sophisticated among the mammals.

Brownell has discussed the evolution of the entire labyrinth[12]. The birds have very short, essentially straight cochlear partitions, curving from 45 to 60 degrees[13]. The owls went further than most birds by evolving a cochlear partition of about ½ turn (180 degrees) and a wider frequency range[14]. With the advent of the mammals, the change in curvature of the cochlea became significant, with a total length frequently reaching 2-4 complete turns. The frequency range of their hearing is directly related to their degree of cochlear partition curvature. As in the case of the owl, the mammals that have developed an active echo-location system have further optimized the curvature of their cochlear partitions at locations associated with specific frequencies. Interestingly, the straight cochlear partition so commonly discussed in hearing research offers no frequency discrimination capability under physiological conditions (Fulton, Section 4.5).

Anson & Donaldson note the cochlear duct or scala media, is initially almost straight in humans. By the seventh week, it consists of one turn. The complete multi-turn configuration is achieved by the eleventh week. Ossification of the otic capsule is complete by the twentieth week. The internal ear is unique in that it reaches maturation (adult size) during the twentieth week of incubation. At that time it has a base diameter of 9 mm and an axial height of 5 mm (page 164). Bredberg has provided similar information concerning the fetus and neonate, including the presence of kinocilia on both OHC & IHC in the four-month-old human fetus (page 54).

The majority of the labyrinth is filled with a specialized (but Newtonian) fluid, the perilymph, that is thought to be obtained from the fluid surrounding the cranial cavity. The labyrinth contains a variety of chambers (shown in darker gray) filled with a second Newtonian fluid, the endolymph, that is more hospitable to some of the specialized structures and mechanisms within the labyrinth. These two fluids are provided with separate sources and reservoirs. The endolymph is not derived from the perilymph. Their compositions are fundamentally different[15,16]. The

reservoirs insure that the chambers occupied by the perilymph and endolymph do not contain any gas-filled space (which is a pathological condition in humans). Since no gas-filled spaces exists in these chambers, no fluid/gas surfaces exists in the cochlea where surface acoustic waves or eddy currents can exist. The sensing operations occur in the endolymph-filled regions of the cochlear partition. The perilymphatic regions of the cochlea appear to act more as a source of acoustic isolation between the bone of the otic capsule and the operations carried out within the endolymphatic regions. It will become clear the bulk of the basilar and tectorial membranes act as inertial masses in hearing. They do not participate actively in the transduction process. It is the LCL surface of the tectorial membrane facing the basilar membrane that is the active acousto-mechanical element within the cochlear duct.

2.2.2 The application of acoustic energy to Hensen's stripe

Many investigators have attempted to describe mechanisms that would cause the energy introduced into the cochlea to travel along a spiral path[17,18]. This paper will present a different approach involving a topographic waveguide (Fulton, Section 4.4.1). Morphologically, such a topographic waveguide is present in the cochlear partition and is known as Hensen's stripe.

The left portion of **Figure 2.2.2-1** provides a semi-scale drawing of the labyrinth based on a mold-model of the scala media prepared by the Born method (a variant of the lost-wax method of forming a physical model of something). This process generates faithful multi-dimensional reproductions of in-situ structures without dissection. The critical importance of this technique will become obvious in the following sections. A similar portrayal of the complete left and right scala media of the chinchilla is shown in Santi[19].

The area of the membrane separating the vestibule and the cochlear duct is quite large in humans. It is estimated from the imagery in Anson & Donaldson to have an area from one third to one-half of the area of the oval window. The surface area of the membrane is approximately perpendicular to the direction to the oval window. Since the acoustic energy passing through the vestibule consists of a compression wave traveling at a nominal 1500 meters/sec, the vestibule can be considered a lumped element from a circuit theory perspective. This would suggest the energy entering the cochlear duct is initially a compression-mode wave. The sensory neurons within the Organ of Corti are unable to process acoustic energy traveling at this speed because of its extremely small size relative to the wavelengths of the energy of interest. The energy must be slowed down by conversion into a surface acoustic wave (SAW) traveling at approximately 1/250th the velocity of sound in a water-based fluid. Such a wave can then be spatially dispersed using techniques well understood in engineering and physics of the current time. The method of propagation slowing will be presented in the next section.

The figure has been divided into three regions to highlight the primary function occurring in each. Following energy collection within the vestibule, the energy is converted into a surface acoustic wave launcher within the caecum of the vestibule. The launcher will be discussed in detail in the next section. Finally, the energy is analyzed in the region conventionally associated with the Organ of Corti. The transition point between the launcher and the analysis regions appears to be defined morphologically by an inflection point in the curvature of the cochlear duct.

The right portion of **Figure 2.2.2-1** consists of three insets representing the cross sections at sections I, II and III in the main figure. They show several important characteristics of the cochlea duct and describes the proposed shape of the gel surface of the tectorial membrane within that duct. No information could be found in the literature concerning the detailed configuration of the tectorial membrane or its gel surface in the area between the Organ of Corti and the vestibule (generally the area labeled stage C2. However, the crease along the side of the mold model indicates where the cochlear partition is located. Based on the crease, the out-of-plane aspects of the basal hook are clearly seen and the apical hook is noted. The sectional views describe a reasonable estimate of the shapes of the tectorial membrane within the scala media. Section I suggests the gel surface occupies most of the volume within the cochlear duct within the vestibule. It would have an area of approximately one square millimeter. It will be shown in the next section, the energy will tend to accumulate on the second surface of the LCL (shading) encountered by the incident energy. Section II shows the twisting of the gel surface within the cochlear duct in order to avoid any curvature of the energy path in the plane of the second gel surface. It also shows the further concentration of the SAW energy in a more limited area above where the Organ of Corti is beginning to form. The letters within the sections are to aid in tracking the form of the duct as it progresses. Section III shows the final form of the cochlear duct and its major components along the active length of the Organ of Corti. The gel surface has attained its final form immediately above the sensory neurons associated with the basilar membrane. The majority of the SAW energy is now confined to the region identified as Hensen's stripe. The cross-section of Hensen's stripe continues to be represented by a shallow convex parabola. The gel surface is now supported by the remainder of the tectorial membrane acting as an inertial mass.

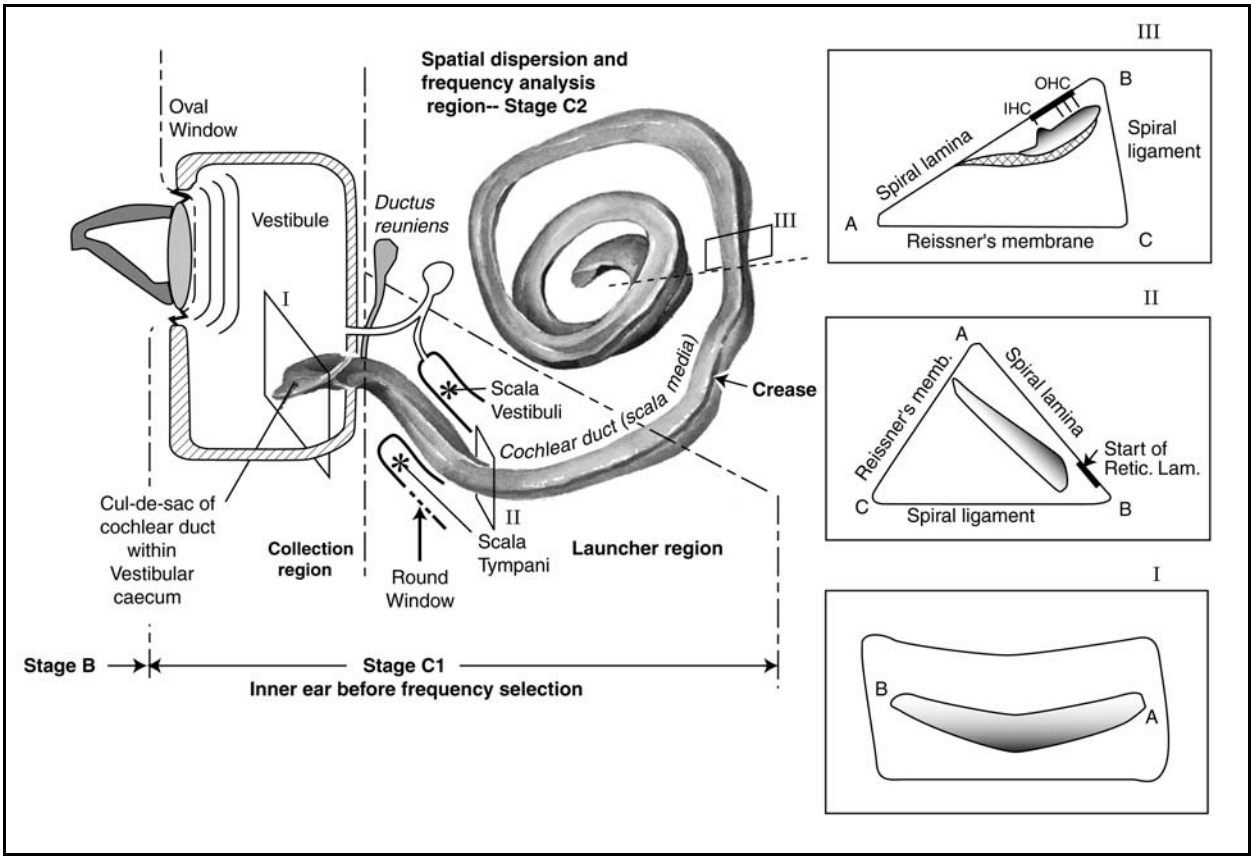

Figure 2.2.2-1 Proposed detail configuration of the vestibule and cochlear duct. Inset I; gel surface of tectorial membrane is the only identifiable feature within the duct Acoustic energy enters the duct from the top. The gel acts as a large area (~1 mm^2) second surface SAW launcher. Energy begins to accumulate at the apex of the convex (parabolic) surface. Inset II; the initial section of the cochlear duct twists to maintain a minimum in-plane curvature of the duct while condensing the energy into an area near the future Organ of Corti. The walls of the duct are shown with their eventual labels. They may not be appropriate at this location. Inset III, the gel surface achieves its final shape and location. It is now associated with the remainder of the tectorial membrane acting as an inertial mass. The energy has been concentrated in Hensen's stripe above the IHC. The limited region between the spiral lamina and the spiral ligament forming the basilar membrane is shown by the heavy line.

2.2.3 The process of launching the surface acoustic wave

This work has identified a crucial functional element of the ear not recognized in the past. This element is the SAW launcher (Latin: launceare) found at the end of the tectorial membrane within the caecum of the vestibule. SAW launchers are extremely simple static devices found widely in nature and used widely in modern engineering and the nondestructive testing of materials. They occur in two basic forms. The simplest, typically associated with wind waves on water, is described as a first surface launcher. The second, typically associated with seismic waves formed during an earthquake, is described as a second surface launcher. **Figure 2.2.3-1** illustrates the operation of the second surface launcher as used in hearing. Energy approaches the launcher at the velocity of a compression wave ($1/k_I$ ~ 1500 m/sec) in the perilymph of the vestibule. The energy departs the launcher as a transverse surface acoustic wave at the interface between the LCL of the tectorial membrane and the endolymph of the scala media at a greatly reduced velocity ($1/k_R$~ 6 m/sec). The ratio between these two velocities is given by the sine of the angle shown.

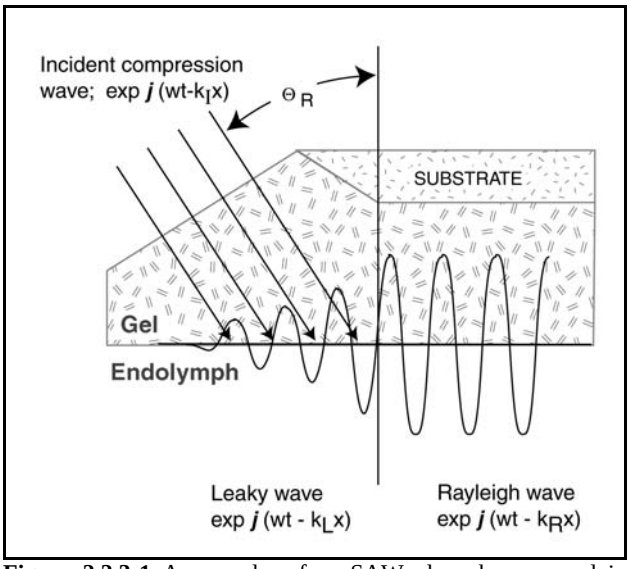

Figure 2.2.3-1 A second surface SAW launcher as used in hearing. The density of the endolymph opposite the gel surface must be of lower density than the gel.

Calculations involving acoustic waves in confined spaces are quite complex and usually require tensor notation mathematics for complete solutions. Shiokawa & Matsui[20] and Auld[21] have provided the necessary mathematics for a full description of compression and transverse acoustic waves using a "simplified notation."

2.3 The mathematical description of Hensen's stripe

Hensen's stripe is a common feature of the tectorial membrane of mammals. While there are systemic differences in the precise shape of the helical character of Hensen's stripe, a baseline can be discerned that is common among these species. This baseline is not as simple as the exponential spiral frequently suggested in the literature, most specifically by Greenwood, and based on empirical data over a limited frequency range[22]. At high frequencies, it can be shown Hensen's stripe is described by a more complex but widely encountered Hankel function (a member of the Bessel function family). However, the apical hook of the cochlea deviates systematically from this function (in the low frequency area). As a result, Hensen's stripe in humans is best described by a modified Hankel function.

Describing Hensen's stripe mathematically requires a nominal cochlea partition. Greenwood provided a description of the variability of cochlear partition length as a footnote (page2604). He noted Bredberg's report of a 28% variation about the mean in the length of the human Organ of Corti. It compared favorably with an earlier report by Hardy of a 33% variation with a standard deviation of 6.8%. For this section, a Standard Human Cochlear Partition will be defined. The data of Stuhlman will be used as a basis after being interpreted as follows. The cochlea will be considered 2 7/8 turns long. A frequency of 15,000 Hz will occur at zero millimeters from the start of in-plane curvature of the cochlear partition. A frequency of 66 Hz will be taken as occurring at 38 mm from the origin. The resulting cochlear partition is 38 mm long instead of the commonly referenced 35 mm.

The short-dashed line in **Figure 2.3.1-1** fits a Hankel function of the first type and zero order to the curve provided by Bredberg. The curve is an excellent fit from his reference point to 720 degrees of rotation. Beyond 720 degrees, the curvature of the stripe increases. This region is frequently described as the apical hook (hamulus) of the cochlea (or cochlear partition). The physical cause of this deviation is unknown but its effect is widely recognized and appears explicitly in the place-frequency-delay characteristic (**Figure 2.4.3-1**). The deviation provides a lower frequency capability within the same physical space than available without the apical hook.

If the simple Hankel function is followed for the first 720 degrees and then an additional term is introduced to account for the hook, a better overall fit is achieved. The long-dashed line in the figure represents a Hankel function modified by an arbitrary factor, $(1-(u/22)^4)$. This modified Hankel function fits the original Bredberg curve to well within the variation in the measured data.

The resulting equation for the active portion of the cochlear partition (Hensen's stripe) as a function of distance, u, is given by;

$$HS = 7.5 \cdot H_0^1(u) \cdot \left(1 - \left(\frac{u}{22}\right)^4\right)$$ for 1.0<u<19. *HS* is the local radius in millimeters from the center of the cochlea (corresponding to the axis of the modiolus), and the figure is rotated until the value at u = 1.0 lies along Bredberg's negative vertical axis.

2.4 Hensen's stripe as a dispersive medium when curved

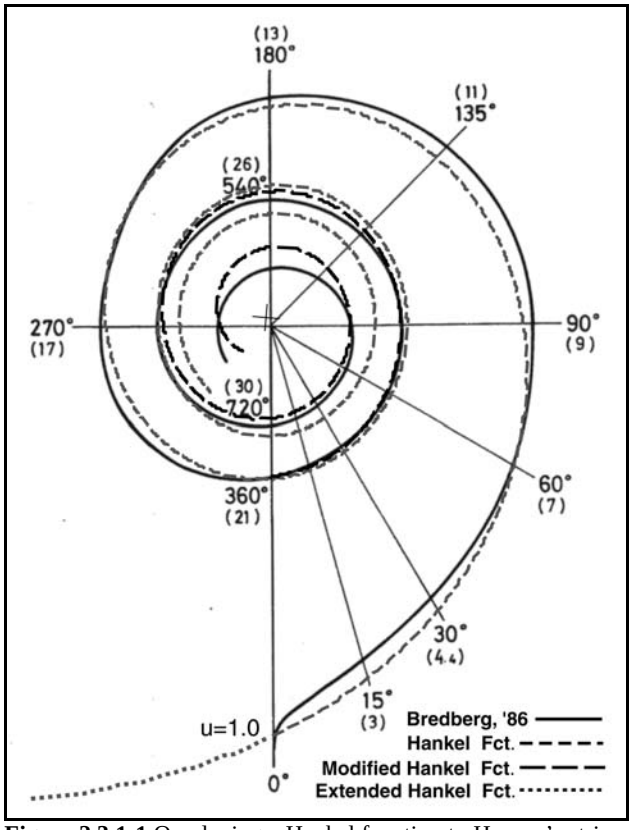

Figure 2.3.1-1 Overlaying a Hankel function to Hensen's stripe. The function is of the first kind and zero order. Its center is indicated by the small cross. The dashed line overlays a figure from Bredberg, 1986. The short-dashed line plots the Hankel function for $0.97 < u < 19$. The dotted line shows the remainder of the Hankel function for $u<0.97$. The numbers in brackets represent the distance from u=0.97. The function fits within the range of data values down to 720 degrees. Beyond 720 degrees, the curvature of the cochlea increases faster than the Hankel function. This area is frequently described as the apical hook. A modified Hankel function that fits the measured data better is shown by the long-dashed line (see text).

The curvature of Hensen's stripe is a critical parameter in hearing. It will be shown that it is this curvature in the plane of the LCL that introduces the frequency dispersive mechanism found in hearing. The mechanism is intrinsic to the propagation of energy along a topographic waveguide that is so curved.

The local curvature of the modified Hankel function can be calculated using standard calculus techniques[23]. However, no simple closed form formula has been found for this function. An alternate numerical computation using the closed form of the modified Hankel function can provide the local radius of curvature as a function of position.

2.4.1 Background

The most important recent applied research applicable to the operation of the cochlea occurred outside the hearing field.

For the reader unfamiliar with surface acoustic waves, several texts are available[24,25,26,27]. The mathematics in Datta have been limited to simple calculus but the descriptions of phenomena are clear. Biryukov et al. have provided an extensive mathematical analysis of surface acoustic waves in more complex situations[28]. They have shown (page 3) that the propagation velocity of simple Rayleigh waves depends only on Poisson's ratio for the substrate. The gel surface of the tectorial membrane, like any gel, exhibits an unusual Poisson's ratio. Long term, a gel cannot resist a tensile force and it will flow. Short-term however, it exhibits a finite Poisson's ratio. Gels are known to support Rayleigh wave oscillations throughout the audio range with very low attenuation. The attenuation of the Rayleigh wave on the surface of an immersed gel is affected by the immersion fluid. The effect can be calculated (Biryukov, page 29).

The propagation of Rayleigh waves on curved surfaces can be described mathematically, but only for selected curvatures in closed form. For substrates other than cylinders, the solutions are usually described in abstract forms. However, Marcatili has found a uniquely appropriate analytical form (discussed in the next section) based on ray tracing.

Marcatili applied the General Wave Equations (GWE) of Maxwell (originally developed in the context of acoustics) to the solution of electromagnetic energy dispersion in a curved dielectric waveguide[29,30]. By extending his analysis from the constant radius to the decreasing radius situation, a description of both the dispersion and the attenuation of a curved non-conducting waveguide can be obtained[31].

2.4.2 The acoustic geometry of the cochlear partition

Figure 2.4.2-1 is a caricature of the nominal acoustic waveguide represented by Hensen's stripe as it is attached to the gel surface of the tectorial membrane. The three known forms of Rayleigh waves are highlighted in this figure. Little is known about the precise cross-section of Hensen's stripe. Micrographs suggest it is about 10 microns wide and on the order of ten microns high. Although much of its external surface is exposed to the endolymph, the acoustic (elastic) properties of the stripe and the endolymph are not reported in the literature.

The reason that the cochlear partition does not perform frequency selection when "uncoiled" should be obvious but will be developed in detail beginning here. In the case of the straight dielectric waveguide of Hensen's stripe (**A**), the energy would tend to propagate primarily as a bounded Rayleigh wave with its phase and energy velocities parallel to the long axis of the waveguide. In the modified Rayleigh surface wave propagation mode, part of the energy is present in the Rayleigh (transverse mode) wave and part is present in the Lamb (in-plane mode) wave (**B**). As the curvature of the waveguide increases in the plane of the LCL, the energy at higher frequencies extends down the side of the waveguide (**C**). When the curvature exceeds a critical frequency-dependent radius, the energy reaches the intersection between the stripe and the gel surface of the tectorial membrane. The surface wave then transitions to the gel surface and proceeds to propagate in a straight line on this flat surface.

> The fact that the curvature of Hensen's stripe is critical to the operation of the cochlear partition in mammals cannot be overemphasized. The question of how a mechanical analog to a totally unwound basilar membrane vibrates is irrelevant to the hearing process.

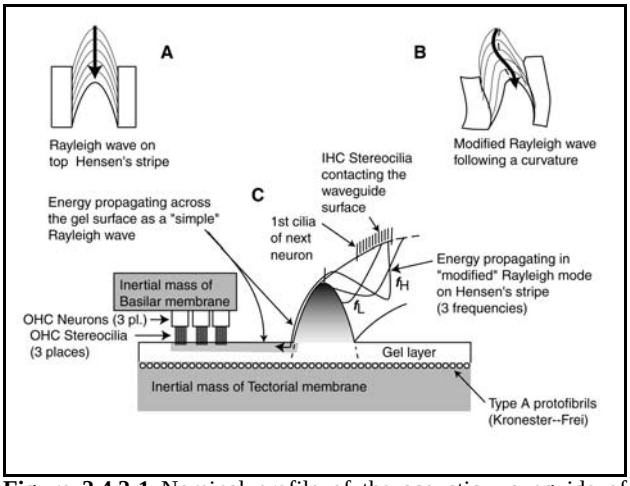

Figure 2.4.2-1 Nominal profile of the acoustic waveguide of hearing. The presence of three different types of Rayleigh wave are shown. The first stereocilia of a IHC group are shown longer only for identification purposes and to define the distance between individual IHC. A; the Rayleigh wave oscillates in the vertical plane and propagates along the top of a straight waveguide. B; with curvature of the waveguide, a modified Rayleigh wave results (with both Rayleigh & Lamb components). C; as curvature increases, the energy travels farther down the sides of the waveguide as a function of frequency until it escapes onto the gel layer surface, where it again propagates in a straight line. The degree of shading indicates the energy density in the waveguide.

It is conventional to describe the energy density of the waveguide under these conditions using the shading shown (**C**). This shading gives a hint at the ability of the stereocilia of the IHC to sense the total energy as a function of frequency at a specific location. It also suggests why the IHC at a given location only show a frequency spectrum up to a certain value. Beyond the point where a given frequency component has transitioned to the gel surface, there is little or no energy in the stripe at that or higher frequencies. An animation of this figure showing the separation of the frequency components more clearly is available at www.hearingresearch.net/anim/energydispersion.htm .

As the dispersed energy propagates as a transverse wave across the surface of the LCL, it encounters the cilia of the OHC. The cilia tend to ride up and down the surface of the acoustic energy wave like a stylus of a phonograph player but the presence of the inertial mass of the tectorial membrane tends to prevent this motion. As a result, the motion of the cilia are absorbed in the piezoelectric portion of the sensory neuron, creating an electrical signal.

2.4.3 Spatial dispersion of energy by a curved waveguide

The above caricature can be described precisely using mathematical functions. Marcatili, and Marcatili & Miller developed the basic mathematics of the curved dielectric waveguide and its surrounding environment in 1969. The key equation is (13) in Marcatili & Miller. It gives the attenuation coefficient, the argument of an exponential, as

$$\alpha_r = c_1 \exp(-c_2 R) \qquad \text{where R is the radius of curvature of the guide.}$$

This equation can be rewritten to include a critical radius, R_c for an argument of 1 neper per meter where this critical radius is frequency sensitive. As a result, the argument can be rewritten as

$$\alpha_r = c_1 \exp(-c_2 R/R_c(f)) \qquad \text{with different values for the constants.}$$

This formulation of an argument of an exponential that is itself an exponential is extremely rare in physics. Many authors have expounded on this mechanism in recent years[32,33,34,35].

By expressing the radius R using the modified Hankel function, and integrating with respect to distance, The point along Hensen's stripe where a specific frequency component must leave the topographic waveguide can be specified.

Figure 2.4.2-2 provides an overview of the process looking down on the cochlear partition parallel to its axis. The figure can be compared to a similar figure developed empirically by Stuhlman (reproduced in Warren[36]). The

energy delivered to Hensen's stripe is dispersed into the gel surface of the tectorial membrane as a function of frequency as shown. This dispersed energy proceeds across the surface of the gel as a simple Rayleigh wave until it is intercepted by and largely transferred to a group of OHC arranged in an echelon parallel to the axis of the wave. The echelon pattern along Hensen's stripe represents the protein molecules in the layer of the TM directly below the LCL. These molecules form an apodizing structure to reduce any tendency of the energy in the Rayleigh wave to disperse laterally.

The OHC neurons are arranged as shown (explicitly for those sensitive to frequencies between 1000 and 2000 Hz) and only intercept a narrow band of frequencies based on the geometry of the cochlear partition and the Marcatili dispersion.

The IHC neurons (not shown) are arranged along Hensen's stripe in order to periodically sample the energy remaining in the stripe. The energy sensed by an IHC has a continually lowering high frequency limit with distance from the basal end of the cochlear partition due to the dispersion process.

2.4.5 The foundation of the place-frequency-delay characteristic

The curvature of the modified Hankel function is directly proportional to the frequency defined by the theoretically derived place-frequency-delay characteristic for a given species. This premise can be demonstrated for a variety of mammals including humans, cats, guinea pigs, dolphins and bats.

Combining the energy-shedding equations of Marcatili with the shape of the cochlea described by a modified Hankel function provides a single equation describing the entire place-frequency relationship in mammals. The key is finding the radius of curvature, R_c, of the modified Hankel function at each point along its course. That value can be used to determine the critical frequency, f_c at that point using the Marcatili-based formulas of **Section 4.4.3**. Several mathematical methods are available for finding the required radii of curvature. The simplest approach appears to involve resolving the Hankel function into separate Bessell and Newmann functions. The differentials of these two functions can be manipulated trigonometrically to find the radius of curvature at each point along the Hankel function. The result is a function that deviates from a straight line at both ends when plotted in a semi-logarithmic space.

Figure 2.4.3-1 graphs the modified Hankel function with respect to distance along the cochlear partition, along with other data. The solid line represents the theoretical place-frequency-delay function of hearing in all species. The constants in the equation were initially adjusted to fit the available data for the cat. The long relatively straight part of this function conforms to the first order approximation of Greenwood, which can also be shown to represent the equation of a simple exponential helix. The available data for multiple species diverges from Greenwood's equation at both high and low frequencies as reported by Evans & Wilson[37] and reproduced by Liberman. The upper portion of the curve is used by a variety of species, specifically dolphins and bats when echolocating.

The fact the theoretical function extends below the zero point on the abscissa emphasizes the arbitrary nature of the morphological limits defined by a specific investigator (and the potential inconsistency among investigators). Schuknecht reproduced a tabulation of place-frequency relationship in humans attributed to Koenig[38,39,40]. The data has been plotted as the dashed line in this figure using an offset abscissa.

The proposed place-frequency-delay characteristic curves down at low frequencies as shown. This region is associated with the apical hook in the previous figures.

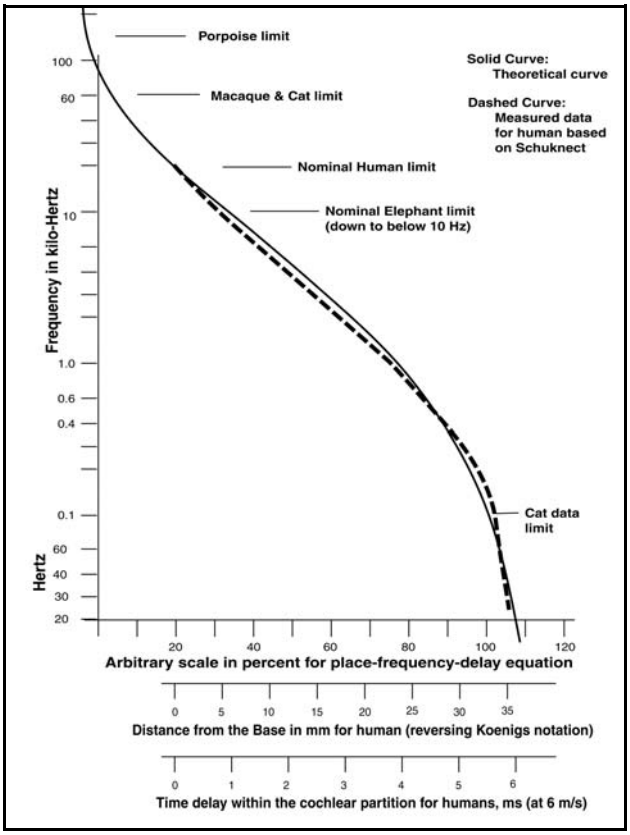

Figure 2.4.3-1 Proposed place-frequency-delay characteristic of the cochlear partition based on a propagation velocity of 6 meters/sec. Solid line, theoretical place-frequency-delay characteristic. Dashed line, measured human data from Schuknect. Also shown, the limits of hearing in various animals as they relate to the theoretical curve. See text.

2.5 Hensen's stripe as a unique low pass filter when curved

Researchers began reporting extraordinarily steep attenuation characteristics on the high frequency side of the best frequency in basilar membrane and neural recordings beginning as early as the 1950's. Most of the early measurements were with respect to the motions of the basilar membrane. The higher and more recent measurements have been associated with individual neural fibers. On the high frequency side, slopes of from 100 to 1000 dB per octave have been reported repeatedly based on many species[41,42]. Rhode gave the precision of his estimate as 100 dB +/– 50 dB per octave, an astounding range from an engineering perspective. No estimate of the error, or even the physiological source, of the 1000 dB per octave value was given. Evans gave plots showing the attenuation slope for dozens of individual neurons with some exceeding 500 dB per octave and many exceeding 100 dB per octave. These values were associated with basilar membrane roll-offs of six dB per octave at low frequencies, building to as much as 80 dB per octave at 10 kHz when associated with fibers having roll-offs on the order of 250 dB *higher*.

No logical explanation for these measured frequency domain characteristics have been offered for this phenomenon since that time. Neither multiple stage RC filters nor any type of resonant circuit can offer attenuation characteristics even approaching the measured values. However, a straightforward explanation is available based on the attenuation parameters associated with a curved topographic waveguide like Hensen's stripe.

The exponential of an exponential and its integral exhibit phenomenal attenuation factors. **Figure 2.5.1-1** shows the attenuation associated with a simple exponential and a single resonant circuit with a Q of 25. Also shown are the attenuations per unit length of a double exponential and the attenuation per unit length of the integral of the double exponential. The differences are dramatic. Whereas the familiar exponential shows an attenuation of 3 dB at an argument of one and 18 dB at an argument of four, and the resonant circuit is only slightly more selective relative to unit frequency, the exponential of an exponential (the "double exponential") shows an attenuation of 7.5 and 236 dB respectively. The slope of the power attenuation at an argument of four is approximately 640 dB per octave. The slope is approximately 40 dB/octave at an argument of two. Even a highly tuned multistage resonant circuit, or an oscillator crystal (with a Q of over 1000) used as a filter, cannot approach this level of attenuation.

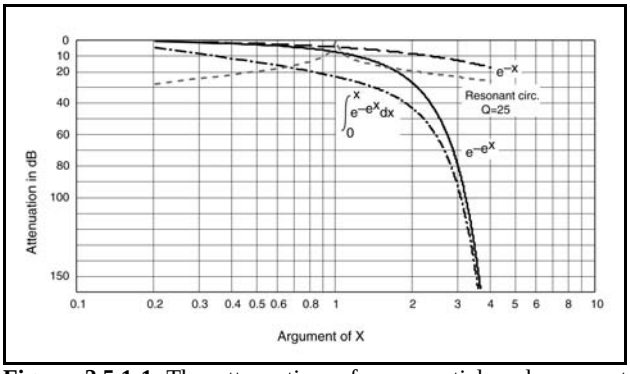

Figure 2.5.1-1 The attenuation of exponential and resonant functions. A simple exponential is shown compared to a resonant circuit with a Q = 25. Also shown are two "double exponentials." The attenuation of the "double exponential" is dramatic compared to the conventional exponential or the resonant circuit. The attenuation associated with the integral of the double exponential is even greater. The curves have been normalized to a common maximum.

The above situations are indicative of the attenuations per unit length possible in a constant radius of curvature configuration. However, the case of interest here is that of a continually changing radius of curvature. Such a configuration calls for a representation of the attenuation coefficient in differential form and integration of that differential form to determine the cumulative attenuation at a given location.

In developing the theory of curved open waveguides, Marcatili & Miller found they were plowing new ground. Paraphrasing Miller from 1964[43], at large radii of curvature, wave propagation in a curved

(dielectric or density) waveguide is virtually the same as in straight guides. However, at radii less than a transition radius something drastic happens. The drastic nature Miller noted is due to the fact the attenuation coefficient of a curved waveguide becomes exponential in character. Rather than solve the difficult mathematics for the cumulative loss as a continuous function of both length and curvature, Marcatili & Miller chose to examine three situations involving curved waveguides of constant radius. Their cases 2 & 3 appear to bracket the conditions found within the cochlear partition. These cases explore an index *difference* (in this case a density difference) between the propagating gel region and the surrounding endolymph region of 0.1% to 1%.

Generalizing their approach, a very complex integral is encountered.

$\int_0^f e^{k \cdot e^{w_x}} dx$ where $w_x = \frac{M \cdot x^{0.5}}{R}$, x equals acoustic frequency, M is a constant and R equals the radius of curvature at the location of interest.

No closed form solution of this integral could be found. However, the method of integration by parts and the conversion of the integrand into a series before integrating both gave similar results[44]. The result consisted of a sum of two closed form terms plus a remainder. Since the terms were found to converge, it was assumed that the remainder terms were small.

Figure 2.5.1-2 shows the unexpected result of this integration when plotted. It shows the predicted normalized attenuation as a function of frequency at three locations along Hensen's stripe in the human cochlea. The attenuation decreases as the frequency corresponding to best frequency is approached. Upon passing the best frequency, the predicted attenuation begins to increase even faster than exponentially. The measured bandpass characteristics of the IHC channels of hearing are in remarkable agreement with this theoretical figure.

The slope of these functions at high frequencies continues to increase without limit, leading to extremely high attenuations per octave. Evans has explored these attenuations beyond the characteristic frequency in detail[45]. He has documented both his auditory nerve measurements and the residual basilar membrane motions of several others. He asserts, "they become steeper with increase in signal level, approaching values of 1000 dB/octave."

The Evans data, and the Bekesy data he references, suggest a low frequency roll-off of about 20 dB per decade but more data would be needed to confirm this slope. The theoretical solution, based on only the first two terms of the partial integration predicts a 10 dB per decade low frequency roll-off.

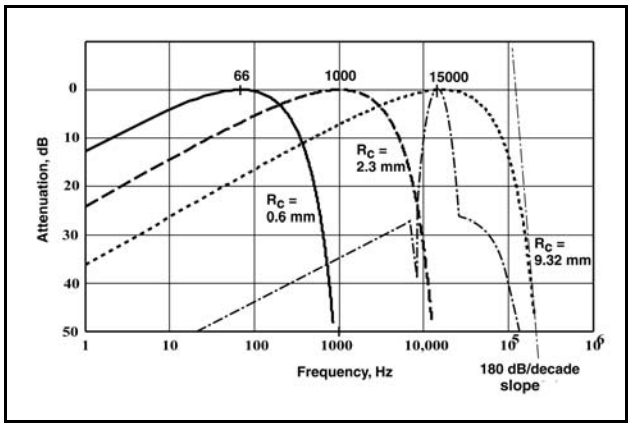

Figure 2.5.1-2 Predicted attenuation for the human cochlea at three radii of curvature along Hensen's stripe. Solid line: radius of curvature of 0.6 mm with optimum performance at 66 Hz (ignoring the effect introduced by the apical hook). The construction line on the right is falling at 180 dB/decade. The rate of attenuation is still increasing at the 50 dB down point for all responses. The dash-dot line represents the attenuation of the OHC channel formed at R_c = 9.32 mm.

Also shown in this figure, but not developed in this paper, is the theoretical attenuation of an OHC channel formed at R_c = 9.32 mm. This characteristic , without the notch at 9 kHz, is formed by concatenating the response of Hensen's stripe at this point (the dotted line) with the narrow bandpass associated with the acoustic geometry of the OHC relative to the dispersed acoustic energy on the surface of the TM. The inflection at 30kHz has also been observed in the experimental literature. The theoretical notch at 9 kHz is observed in laboratory experiments involving a phase sensitive summation of the IHC and OHC channels. It has been labeled Kiang's notch in the literature.

The data of Manly, Yates & Koppl[46] and many papers by the Kiang team can be overlaid by the functions developed above to show how successfully they describe the empirical situation (Fulton, figure 4.5.2-4).

2.6 Alternate acoustic paths through the cochlea

Figure 2.6.1-1 describes different potential signal paths through the complete inner ear. The previously proposed paths incorporate the basilar membrane as an active participant. However, these paths have not accounted for the coupling loss between the oval window and the basilar membrane, or explained how a signal below the noise level (due to Brownian motion) is recovered and amplified

back to the measured energy level at the cilia of the sensory neurons. The signal path defined here does not encounter these problems. The signal is efficiently transferred from the oval window to the LCL and then to the appropriate sensory neurons with the bulk of the tectorial membrane and the bulk of the basilar membrane acting as inertial masses. These masses each receive a few percent of the total energy available, in accordance with measurements.

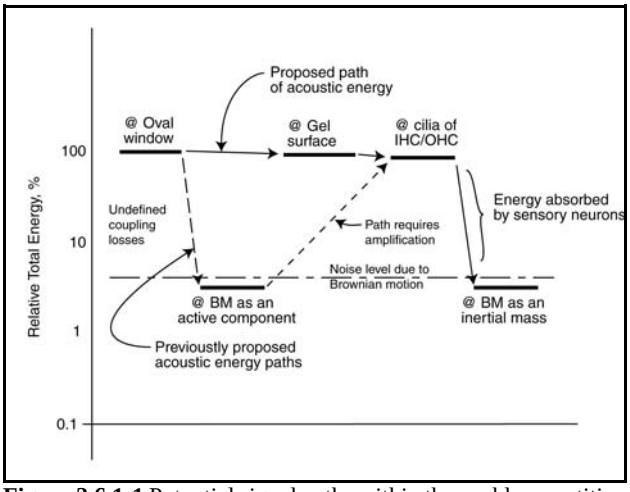

Figure 2.6.1-1 Potential signal paths within the cochlear partition (Organ of Corti). Solid arrows show paths proposed in this theory. Dashed arrows represent the earlier proposals. No low-loss acoustic path between the oval window and the basilar membrane has been described in the literature. Earlier proposals require a mechanical cochlear amplifier to raise the signal level above the measured level of the basilar membrane. Alternate earlier proposals require an undocumented connection between the scala vestibuli and the vestibule of the labyrinth.

Derivations of more detailed structural mechanical models of the system focused on both the longitudinal and lateral propagation of energy on the LCL of the tectorial membrane are available (Fulton, Section 4.6.1). Animations related to these models are available at www.hearingresearch.net/anim/longstructuralmodel.htm and www.hearingresearch.net/anim/lateralstructuralmodel.htm respectively.

4 Conclusion

The surgical literature has described an acoustic path involving the tectorial membrane, and particularly Hensen's stripe as the principle element of acoustic energy propagation within the cochlea with the bulk of the tectorial membrane and the basilar membrane playing ancillary roles as inertial masses.

Analyses based on Hensen's stripe as the principle element of acoustic energy propagation have led to:
• unique and specific descriptions of separate sensory roles for the OHC and the IHC.
• A unique description of the complete place-frequency-delay characteristic of human hearing.
• The first explanation in the literature for the extremely high attenuation at acoustic frequencies higher than best frequency for the OHC and IHC.

The spatial dispersion from a curved waveguide is the only mechanism known to physics that can achieve these high attenuations per octave with increasing frequency above the peak response frequency. The fact this mechanism predicts both the low pass characteristic and the extremely high attenuation per octave at high frequencies measured in the cochlea is strong support for the validity of this theory of cochlear operation.

Propagation via Hensen's stripe within the cochlear partition negates the need for a mechanical amplifier to raise the amplitude of basilar membrane vibrations.

- - - -

Theoretical descriptions of the place-frequency, and expanded place-frequency-delay, characteristics of human hearing are presented along with a theoretical description of the bandpass characteristic of the IHC related signaling channels as a function of the curvature of Hensen's stripe within the cochlea. The latter description includes the mechanism leading to uniquely high attenuation associated with the high frequency skirt of the bandpass characteristic.

- - - -

Replacing the putative, and poorly supported, resonance mechanism within the cochlear partition with a dispersion mechanism leads to remarkable agreement with the empirical data base and predicts many phenomena of hearing not previously explained.

The arrangement of the vestibule of the labyrinth is compatible with the launch of a surface acoustic wave on the tectorial membrane within the cochlear partition.

The measured acousto-mechanical properties of the liquid-crystalline surface of the tectorial membrane facing the reticular lamina are compatible with the measured acoustic propagation velocity in mammalian, and human, hearing. (3-10 meters/sec.).

14 Mechanics of Hearing

Table of Contents

Hensen's Stripe as a topographic waveguide
defines the roles of the OHC & IHC 1

Abstract: 1

1. Introduction 1

2. The operation of the vestibule of the labyrinth and cochlear partition 1
2.1 The properties of the liquid crystalline layer of the tectorial membrane 2
2.2 The acoustic path between the vestibule and the cochlear partition 2
2.2.1 Evolution and development of the cochlea and cochlear partition 3
2.2.2 The application of acoustic energy to Hensen's stripe 4
2.2.3 The process of launching the surface acoustic wave 5
2.3 The mathematical description of Hensen's stripe 6
2.4 Hensen's stripe as a dispersive medium when curved 7
2.4.1 Background 7
2.4.2 The acoustic geometry of the cochlear partition 7
2.4.3 Spatial dispersion of energy by a curved waveguide 8
2.4.5 The foundation of the place-frequency-delay characteristic 9
2.5 Hensen's stripe as a unique low pass filter when curved 10
2.6 Alternate acoustic paths through the cochlea 12

4 Conclusion 12

List of Figures

Figure 2.2.1-1 A caricature of the labyrinth with the cochlea acoustically isolated from the vestibule 3
Figure 2.2.2-1 Proposed detail configuration of the vestibule and cochlear duct 5
Figure 2.2.3-1 A second surface SAW launcher 5
Figure 2.3.1-1 Overlaying a Hankel function to Hensen's stripe 6
Figure 2.4.2-1 Nominal profile of the acoustic waveguide of hearing 8
Figure 2.5.1-1 The attenuation of exponential and resonant functions 11
Figure 2.5.1-2 Predicted attenuation for the human cochlea at three locations along Hensen's stripe 11
Figure 2.6.1-1 Potential signal paths within the cochlear partition 12

16 Mechanics of Hearing

Endnotes

1. Hawkins, J. E. jr. (1988) Auditory physiological history: a surface review *In* Jahn, A. & Santos-Sacchi, J. *ed*. Physiology of the Ear NY: Raven Press pg 26. Repeated in 2001 edition

2. Fulton, J. (2008a) Hearing: A 21st Century Paradigm. Victoria, BC. CA: Trafford

3. Fulton, J. (2008b) www.hearingresearch.net

4. Kronester-Frei (1978) Ultrastructure of the different zones of the tectorial membrane *Cell Tiss Res* vol. 193, pp 11-23

5. Kronester-Frei, A. (1979) The effect of changes in endolymphatic ion concentrations on the tectorial membrane *Hear Res* vol. 1, pp 81-94

6. Lim, D. (1972) Fine morphology of the tectorial membrane *Arch Otolaryngol* vol 96, pp 199-215

7. Thalmann, I. Thallinger, G. Crouch, E. et al. (1987) Composition and supramolecular organization of the tectorial membrane *Laryngoscope* vol 97, pp 357-367

8. Hasko, J. & Richardson, G. (1988) The ultrastructural organization and properties of the mouse tectorial membrane matrix *Hear Res* vol 35, pp 21-38

9. Zwislocki, J. Chamberlain, S. & Slepecky, N. (1988) Tectorial membrane I: static mechanical properties *in -vivo*. *Hear Res* vol 33, PP 207-222

10. Ghaffari, R. Aranyosi, A. & Freeman, D. (2007) Longitudinally propagating traveling waves onf the mammalian tectorial membrane *PNAS*, vol 41, pp 16510-16515

11. Donaldson, J. Lambert, P. Duckert, L. & Rubel, E. (1992) Anson & Donaldson: Surgical Anatomy of the Temporal Bone, 4th Ed. NY: Raven Press, pages 71, and 267-277

12. Brownell, W. (2006) the piezoelectric outer hair cell: bidirectional energy conversion in membranes *In* Nuttall, A. et. al. *eds*. Auditory Mechanisms: Processes and Models. Singapore: World Scientific pp 176-186

13. Cotanche, D. & Corwin, J. (1990) Stereociliary bundles reorient during hair cell development and regeneration in the chick cochlea *Hear Res* vol 52, pp 379-402

14. Koppl, C. Achenback, A Sagmeister, T. & Schebelle, L. (2006) Development of micromechanically-relevant hair-cell properties: Late maturation of hair-cell orientation in the basilar papilla of birds *In* Nuttall, A. et. al. *eds*. Auditory Mechanisms: Processes and Models. Singapore: World Scientific pp 377-383

15. Salt, A. & Konishi, T. (1986) The cochlear fluids: perilymph and endolymph *In* Altschuler, R. Bobbin, R. & Hoffman, D. *eds*. Neurobiology of Hearing: the cochlea. NY: Raven Press pp 109-122

16. Rauch, S. & I. (1974) Physico-chemical properties of the inner ear especially ionic transport *In* Keidel, W. & Neff, W. *eds*. Auditory System: Anatomy: Physiology (Ear). NY: Springer-Verlag pp 647-682

17. Van Duzer, T. (1970) Lenses and graded films for focusing and guiding acoustic surface waves *Proc IEEE* vol 58(8), pp 1230-1237

18. Jiao, B. & Zhang, J. (1999) Torsional modes in piezo hielical springs *IEEE Trans Ultrasonics, Ferro, Freq Control* vol 46(1) pp 147-151

19. Santi, P. (1986) Organ of Corti surface preparations for computer-assisted morphometry Hear Res vol 24, pp 179-187

20. Shiokawa, S. & Matsui, Y. (1995) The dynamics of SAW streaming and its application to fluid devices *In* George, E. et al. *ed*. Materials for Smart Systems. Pittsburgh, PA: Materials Research Society pp 53-64

21. Auld, B. (1973) Acoustic Fields and Waves in Solids, Volume 1. NY: John Wiley & Sons

22. Greenwood, D. (1990) A cochlear frequency-position function for several species–29 years later *J Acoust Soc Am* vol 87(6), pp 2592-2605

23. Kells, L. (1950) Analytic Geometry and Calculus. NY: Prentice-Hall Articles 123-125 & 233.

24. Hashimoto, K-Y. (2000) Surface Acoustic Wave Devices in Telecommunications. NY: Springer

25. Oliner, A. ed. (1978) Acoustic Surface Waves. NY: Springer-Verlag.

26. Datta, S. (1986) Surface Acoustic Wave Devices. Englewood Cliffs, NJ: Prentice-Hall

27. Auld, B. (1985) Rayleigh wave propagation *In* Ash, E. & Paige, E. *eds*. Rayleigh-Wave Theory and Application. NY: Springer-Verlag pp 12-25

28. Biryukov, S. Gulyaev, Y. Krylov, V. & Plessky, V. (1995) Surface Acoustic Waves in Inhomogeneous Media. NY: Springer-Verlag

29. Marcatili, E. (1969) Bends in optical dielectric waveguides *BSTJ* vol 48, pp 2103-2132

30. Marcatili, E. & Miller, S. (1969) Improved relations describing directional control in electromagnetic wave guidance *BSTJ* vol 48, pp 2161-2181

31. Fulton, J. (2008) Biological Hearing: A 21st Century Paradigm. Victoria, BC, CA: Trafford Sections 4.4.3–4.5

32. Smit, M. Pennings, E. & Blok, H. (1993) A normalized approach to the design of low-loss optical waveguide bends *J Lightwave technol* vol. 11(11), pp 1737-1742

33. Melloni, A. Carniel, F. Costa, R. & Martinelli, M. (2001) Determination of bend mode characteristics in dielectric waveguides *J Lightwave technol* vol 19(4), pp 571-577

34. Hiremath, K. Hammer, M. Stoffer, R. & Ctyroky, L. (2005) Analytic approach to dielectric optical bent slab waveguides *J Optic Quant Electr* vol 37(1-3), pp 37-61

35. Marcuse, D. (1982) Light Transmission Optics, 2nd Ed. NY: Van Nostrand Reinhold

36. Warren, R. (1982) Auditory Perception: A New Synthesis. NY: Pergamon Press pp 2-12

37. Evans, E. & Wilson, J. (1977) Cochlear frequency map for the cat *In* Evans, E. & Wilson, J. *eds*. Psychophysics and Physiology of Hearing. NY: Academic Press pp 69+

38. Otte, J. Schuknect, H. & Kerr, A. (1978) Ganglion cell populations in normal and pathological human cochleae *Laryngol* vol 88(8), pp 1231-1246

39. Schuknect, H. (1974) Pathology of the Ear. Cambridge, MA: Harvard University Press Table 3.2

40. Koenig, W. (1949) A new frequency scale for acoustic measurements Bell Laboratory Record, pg 299+

41. Kiang, N. (1965) Discharge Patterns of Single Fibers in the Cat's Auditory Nerve. Cambridge, MA: MIT Press research monograph #35

42. Rhode, W. (1970) Observations of the vibration of the basilar membrane in squirrel monkeys using the Mossbauer technique *J Acoust Soc Am* vol. 49(4), pt 2, pp 1218-1231

43. Miller, S. (1964) Directional control in light-wave guidance *BSTJ*. vol 43(4) pp 1727-1739

44. Integration available from the author upon request.

45. Evans, E. (1975) Cochlear nerve and cochlear nucleus *In* Keidel, W. & Neff, W. *eds*. Handbook of Sensory Physiology: Auditory Systems, volume 5.2, pages 1–108 Berlin: Springer pg 15

46. Manley, G. Yates, G. & Koppl C. (1988) Auditory peripheral tuning: evidence for a simple resonance phenomenon in the lizard Tiliqua *Hear Res* vol 33(2), pp 181-189